
STATISTICAL, NONLINEAR,
AND SOFT MATTER PHYSICS

Multiple-Quantum NMR Spectroscopy and Quantum Information Spreading Control in the Spin Systems of Solids

V. E. Zobov^{a,*} and A. A. Lundin^{b,**}

^a*Kirensky Institute of Physics, Federal Research Center KSC SB RAS,
Krasnoyarsk, 660036 Russia*

^b*Semenov Federal Research Center for Chemical Physics, Russian Academy of Sciences,
Moscow, 117977 Russia*

**e-mail: rsa@iph.krasn.ru*

***e-mail: ya-andylun2012@yandex.ru*

Received April 10, 2022; revised May 15, 2022; accepted May 16, 2022

Abstract—Multiple-quantum (MQ) solid-state NMR spectroscopy allows the growth of multiple-spin correlations and, thus, the spreading of quantum information in the object under study to be observed. Recently, in [11] it was proposed to control this process through a controlled perturbation added to the effective Hamiltonian that causes degradation of correlated spin clusters with a rate determined by the number of spins K in a cluster. However, this perturbation can also lead to degradation whose rate is determined by the coherence order M . In this paper, to investigate the influence of a small added perturbation, we used an expansion into orthogonal operators that allowed the cluster size distribution to be taken into account. In our calculations we realized a simple model with known amplitudes of the expansion into a complete set of orthogonal operators in the absence of a perturbation. We performed numerical calculations of the “preparation time” dependences of the MQ spectra, their second moments, and the coherence orders at which the MQ spectra decrease by a factor of e as well as the average correlated spin cluster sizes \bar{K} . The coherence-order-dependent contribution to the degradation is shown to change the shape of the MQ spectrum. In particular, as the preparation time increases, the MQ spectrum can be stabilized, while the growth of \bar{K} is retained. Due to the change in the shape of the MQ spectrum, the relations of its characteristics to the number \bar{K} change compared to those for the Gaussian function (traditionally used to process the experiments). These changes should be taken into account when studying the spreading of quantum information through MQ spectroscopy.

DOI: 10.1134/S1063776122110139

1. INTRODUCTION

The active development of multiple-quantum (MQ) NMR spectroscopy, which appeared as a consequence of the intensive development of multiple-pulse NMR [1], began in the late 1970s—early 1980s as a powerful and often virtually irreplaceable tool for a practical study of the structure of macromolecules (for example, proteins), clusters, and local structures located on surfaces [2], in liquid crystals [3], nanosized cavities [4], etc. The basis for MQ spectroscopy is the observation of the behavior of multiple-spin/multiple-quantum coherent states. These states arise under the action of internal interactions in conditions when the nuclear spin subsystem of a material in a condensed state is irradiated by a certain sequence of radio-frequency pulses [1, 5, 6].

The emerged possibility of an experimental study of the development of multiple-spin correlations with time through MQ NMR spectroscopy turned out to be

in demand in the statistical physics of irreversible processes [7] and in studying the physical processes needed for the development of quantum informatics (the creation of quantum registers) [8]. The point is that the system of nuclear magnetic moments (spins) of a solid observed by NMR methods serves as a good example of a closed system and, as is well known, quantum information in a closed system is preserved with time [8]. At the same time, this information initially localized in single-particle (single-spin) states is redistributed over a set of degrees of freedom, which can be reflected by the appearance of time correlation functions (TCFs) with a very complex structure.

The spreading of quantum information over a multiparticle system is called scrambling (see, e.g., [9–11]). Four-operator TCFs belonging to the class of TCFs abbreviated to OTOC (out-of-time-order correlator) (see, e.g., [12–15]) are commonly used for a theoretical description of these processes (scrambling):

$$C(t) = \langle W^+(t)V^+(0)W(t)V(0) \rangle_{\beta}.$$

Here, $V(0)$ and $W(0)$ are two commuting operators, while the time dependence is determined by an ordinary unitary operator with the system's Hamiltonian in the exponent. The angle brackets $\langle \dots \rangle_{\beta}$ denote a statistical average. The OTOC TCFs related to the information entropy contain specific information about the most intimate processes occurring in the multiparticle system: multiparticle entanglement, localization in the many-body system, the development of quantum chaos, and so on, up to some aspects of black hole physics [12, 13, 15] (for example, the Hawking radiation). It should be noted that in experimental studies MQ NMR of multiple-spin systems has a number of noticeable advantages compared to other multiparticle systems, such as ultracold neutral atoms [12] or trapped ions [13]. The point is that the TCFs used (arising in a natural way during experiments) in MQ spectroscopy belong to the class of OTOCs, i.e., these are four-particle TCFs containing (by definition) a time-reversed stage of evolution [16, 17]. It should be said that among the set of various four-particle OTOC-type TCFs arising in MQ NMR, the second moment of the MQ spectrum plays a very significant role [18, 19] due to two circumstances. Its value determines a lower bound on the Fisher criterion [20–22] for quantum information that represents a measure of entanglement. In addition, the second moment of the MQ spectrum is a quantity directly measurable in an experiment and, consequently, allows the OTOC TCF corresponding to it to be determined experimentally [23].

Constructing a consistent theory for the shape of the MQ NMR spectrum of solids and rigorously calculating the corresponding TCFs is an extremely complex multiparticle and so far very poorly studied problem. In the traditional statistical model [5, 6] the following Gaussian distribution was obtained for the distribution of coherences of various orders M in the MQ spectrum using a very simple algebraic estimate of the number of transitions between various levels of large clusters:

$$G_M(T) = \frac{1}{\sqrt{\pi \bar{K}(T)}} \exp\left(-\frac{M^2}{\bar{K}(T)}\right). \quad (1)$$

The second moment (variance) of the distribution in this model $\bar{K}(T)/2$ is determined by the average number of spins $\bar{K}(T)$ between which a dynamic correlation was established in the preparation time T . This number, called the number of correlated spins or the effective (average) cluster size, increases with preparation time T .

In [19] we showed that for three-dimensional nuclear spin systems with a secular dipole–dipole interaction (or with an effective two-spin/two-quantum interaction (see below)) the second MQ NMR moment, which determines the number of correlated

spins, increases in the ideal case (in the absence of any perturbations) exponentially with time T . The results obtained in [19] allowed us, in particular, to explain the experimental data from [24–28] on the observation of the emergence of correlated spin clusters containing $\sim 10^5$ particles.

In a real situation, the growth of correlated spin clusters is limited due to the various processes causing cluster degradation. To investigate them, in [11, 27, 29, 30] a perturbation whose value was specified by the experimenters themselves was added to the effective Hamiltonian in the preparation period. It was found that as the perturbation increases, the growth of the number \bar{K} with time T slows down and can stop altogether. On this basis, the authors of [11] proposed a method for controlling the growth of the number \bar{K} and, thus, developed a technique for controlling the spreading of quantum information through a controlled perturbation. To describe these processes accompanying the development of clusters, a model was proposed in [31] that is based on the equations for the amplitudes of clusters of different sizes taken from [32]. A diffusive cluster growth was assumed within this model (which, generally speaking, is improper, see [19]), while the rate of its degradation was determined exclusively by the cluster size.

It should be pointed out that in experiments the average number of correlated spins \bar{K} is usually extracted from the width of the observed MQ spectrum by assuming that this can be done in accordance with the relations derived for the ideal case due to the weakness of the external perturbations. The described technique was also used to process the experimental results by the authors of [11, 27, 29]. It should be noted that this assumption, nevertheless, needs to be justified, since the perturbation can change the shape of the MQ spectrum itself. For example, in [24] it was experimentally established that the cluster degradation rate depends not only on its size, but also on the coherence order. The calculations and estimates performed by us previously [33–35] showed that the rapid decay of spectral components with large coherence orders could lead to stabilization of the MQ spectrum as the time T increases, despite the ongoing growth of the number of correlated spins \bar{K} . Thus, this physical degradation mechanism omitted in [11, 31] affects significantly the observed cluster size and it has to be investigated when improving the quantum information spreading control methods being developed.

In this paper, through an expansion of the sought-for TCFs into an infinite set of orthogonal operators and using some known facts for traditional model systems [19, 35–37], we obtained the series in growing number of spins in a cluster for \bar{K} for the MQ spectrum and its various characteristics. We took into account both physical cluster degradation mechanisms: both dependent on the number of spins in a

cluster and dependent on its coherence order. Numerical calculations were performed for various values of the parameters appearing in the final expressions.

The paper has the following structure. In Section 2 we present the general formulas and series for the ideal case where there are no perturbations leading to cluster degradation. In Section 3 we derive the expressions in which the cluster degradation processes are taken into account. In Section 4 we present the results of our numerical calculations and their discussion. Section 5 presents a brief conclusion. Finally, in the Appendix we consider the peculiarities of our calculations for clusters with a small number of spins.

2. THE HAMILTONIAN AND BASIC EQUATIONS FOR THE CORRELATION FUNCTIONS

The secular part of the internuclear dipole–dipole interactions in nonmetallic diamagnetic solids solely responsible for the dynamics of the spin system consisting of light nuclei, such as, for example, protons or ^{19}F nuclei, under NMR conditions is [38]

$$H_{dd} = \sum_{i \neq j} b_{ij} S_{zi} S_{zj} - \frac{1}{2} \sum_{i \neq j} b_{ij} S_{+i} S_{-j}, \quad (2)$$

where $b_{ij} = \gamma^2 \hbar (1 - 3 \cos^2 \theta_{ij}) / 2r_{ij}^3$, \mathbf{r}_{ij} is the vector connecting spins i and j , θ_{ij} is the angle formed by the vector \mathbf{r}_{ij} with the constant external magnetic field, γ is the gyromagnetic ratio, $S_{\alpha i}$ is the α component ($\alpha = x, y, z$) of the vector spin operator at site i , $S_{+i} = S_{xi} + iS_{yi}$, $S_{-i} = S_{xi} - iS_{yi}$. Here and below, the energy is expressed in frequency units.

In traditional experiments using NMR the spin temperature usually exceeds considerably the energy of the Zeeman and other interactions in the spin system. Therefore, we, as usual, will restrict our study to the time correlation functions (TCFs) in the high-temperature approximation. The equilibrium high-temperature density matrix in a strong static magnetic field H_0 is described by the expression [38]

$$\rho_{\text{eq}} \approx 1 + \frac{\gamma \hbar H_0}{kT} \sum_{j=1}^N S_{zj},$$

where k is the Boltzmann constant, T is the temperature, and N is the total number of spins in the sample.

The Hamiltonian (2) is the basic one for “spin alchemy,” transforming into other Hamiltonians of interest to the researcher under the influence of radio-frequency pulses [1]. For example, in traditional MQ NMR [1–6] the Hamiltonian (2), as a rule, turns into a two-spin/two-quantum Hamiltonian H_{DQ} of the form

$$H_{DQ} = -\frac{1}{4} \sum_{i \neq j} b_{ij} (S_{+i} S_{+j} + S_{-i} S_{-j}). \quad (3)$$

Under the action of the nonsecular (with respect to equilibrium magnetization) Hamiltonian (3), the initial magnetization is transferred to various TCFs with a fairly complex structure dependent on the product of various numbers (K) of spin operators (multiple-spin correlations). In other words, the equilibrium density matrix in a strong magnetic field ρ_{eq} turns into a non-equilibrium density matrix, which is convenient to represent as a sum of the off-diagonal elements ρ_M with a certain difference of M magnetic quantum numbers called multiple-quantum coherences (M is the coherence order):

$$\rho(t) = \exp\{iHt\} \rho_{\text{eq}} \exp\{-iHt\} = \sum_M \rho_M(t),$$

$$\rho_M(t) = \sum_{K=|M|}^{K=N} \sum_{\{i\}} \sum_q g_{KMq\{i\}}(t) |KMq\{i\}\rangle,$$

where $|KMq\{i\}\rangle$ is the basis operator in which K single-spin operators form a product coupling Zeeman states differing by M units. The index q numbers different basis states with the same values of K and M . At time $t = T$ the emerged coherences are marked with a phase shift φ . The emerging phase shift is proportional to $M\varphi$, where M is an integer. Thus, the K -spin correlations, depending on M , are also distinguished by the number of quanta ($M \leq K$) [1, 3, 5, 6]. Then, a new pulse sequence changing the sign of the mentioned nonsecular Hamiltonian (3) is applied to the system and, thus, “time reversal” is performed [39, 40], as a consequence of which the system evolves “backward.” At time $t = 2T$ a Loschmidt echo is observed. Its amplitude $\Gamma(\varphi, T)$ depends on φ and may be written as follows:

$$\Gamma(\varphi, T) = \frac{\text{Tr}\{U_2^+(T) U_\varphi U_1(T) S_z U_1^+(T) U_\varphi^+ U_2(T) S_z\}}{\text{Tr}\{S_z^2\}}, \quad (4)$$

where $U_{1(2)}(t)$ is the evolution operator with an “operating Hamiltonian (for example, H_{DQ} from Eq. (3)).” The indices 1 and 2 denote, respectively, the forward and backward evolution with time, $U_\varphi = \exp(i\varphi S_z)$ is the rotation operator by an angle φ around the z axis, and S_z is the z component of the total spin of the nuclear system. The amplitude of the echo $\Gamma(\varphi, T)$ is measured with the help of a $\pi/2$ pulse rotating the magnetization into a plane perpendicular to the external magnetic field. The experiment is repeated many times with different phase shifts φ of irradiating pulses for each duration T of the preparation period. The two-dimensional MQ NMR spectrum $G_M(T)$ that is a function of two variables, M and T , can be obtained through a Fourier transform of the TCF $\Gamma(\varphi, T)$ with respect to the variable φ .

An important characteristic of the MQ spectrum is its second moment [11, 18, 19, 21, 23, 31], for which through relation (4) we find:

$$\begin{aligned} \langle M^2 \rangle &= \sum_M M^2 G_M(t) = -d^2 \Gamma(\varphi, T) / d\varphi^2|_{\varphi=0} \\ &= \frac{\text{Tr}\{[S_z, U_1(T) S_z U_1^\dagger(T)] [U_2(T) S_z U_2^\dagger(T), S_z]\}}{\text{Tr}\{S_z^2\}}. \end{aligned} \quad (5)$$

Both TCF (4) and (5) belong to the class of OTOCs considered in the Introduction.

To solve the formulated problem of calculating the shape of the MQ spectrum and the average size of a cluster of correlated spins, as shown in [35], it is appropriate to use an expansion of the time-dependent spin operators into a complete set of orthogonal operators [41]:

$$S_z(t) = \sum_{j=0}^{\infty} A_j(t) |j\rangle \quad (6)$$

and to investigate the changes in the amplitudes of this expansion

$$A_j(t) = \frac{\langle j | S_z(t) \rangle}{\langle j | j \rangle} \quad (7)$$

due to a perturbation. Such expansions have also been repeatedly used in nonequilibrium statistical mechanics previously (see, e.g., [19, 42–46]) to describe a variety of TCFs. The angle brackets reflect taking a scalar product [41], i.e., in fact, calculating a statistical average. The latter under conditions of the high-temperature approximation means simply a calculation of the trace of the corresponding product of operators. The Gram–Schmidt procedure [19, 37, 41, 47] is commonly used in orthogonalization. Below, we give several vectors

$$\begin{aligned} |0\rangle &= S_z, \quad |1\rangle = i[H, |0\rangle], \\ |j+1\rangle &= i[H, |j\rangle] + v_{j-1}^2 |j-1\rangle \quad \text{for } j \geq 1, \\ v_j^2 &= \langle j+1 | j+1 \rangle / \langle j | j \rangle. \end{aligned} \quad (8)$$

Since each commutation with the two-spin interaction Hamiltonian adds at most one spin operator to the product of the spin operators of which the vector $|j\rangle$ consists, we will consider the orthogonal operator $|j\rangle$ as an operator representing a cluster of $K = j + 1$ spins. Such a representation (see, e.g., [35, 37, 45, 48]) is justified in the presence of a large number of neighbors surrounding each (any) spin in the lattice adequate for most ordinary solids (adamantine, fluorite, etc.). In this approximation we will write the MQ spectrum in the absence of perturbations as a sum of the MQ spectra g_{KM} (see the Appendix) from clusters of different sizes [35, 37]:

$$G_M(T) = \sum_{K=|M|}^{\infty} g_{KM} P(K, T), \quad (9)$$

where

$$P(K, T) = A_{K-1}^2(T) \langle K-1 | K-1 \rangle / \text{Tr}(S_z^2) \quad (10)$$

is actually the distribution in the number of clusters with $K = j + 1$ spins, since the following condition is fulfilled for it:

$$\Gamma(\varphi = 0, T) = \sum_{K=1}^{\infty} P(K, T) = 1.$$

In the adopted representation, the average cluster size equal to twice the second moment of the MQ spectrum (9) is described by the series

$$\bar{K}(T) = \sum_{K=1}^{\infty} K P(K, T). \quad (11)$$

For dense spin systems, such as adamantine or fluorite, which are characterized by an exponential growth of \bar{K} , we will use a well-known expression for the sought-for amplitudes [19, 35, 36]:

$$\begin{aligned} A_0(t) &= \frac{1}{\cosh^2(t/\sqrt{2})}, \\ A_j(t) &= \frac{1}{\cosh^2(t/\sqrt{2})} \frac{\tanh^j(t/\sqrt{2})}{j!}. \end{aligned} \quad (12)$$

Here and below, the time is expressed in units of the inverse second moment ($1/\sqrt{m_2}$) of the function $A_0(t)$. For these amplitudes we have

$$P(K, T) = \frac{(\tanh^2(T/\sqrt{2}))^{K-1} K}{\cosh^4(T/\sqrt{2})}, \quad (13)$$

$$\bar{K}(T) = 1 + 2 \sinh^2(T/\sqrt{2}). \quad (14)$$

3. THE LOSS OF COHERENCE IN THE SYSTEM AND ITS INFLUENCE ON THE MQ SPECTRUM

As has already been noted above, in the absence of any external perturbations, an unlimited growth of \bar{K} with a time dependence very close to the exponential one is to be expected [19]:

$$\bar{K}(t) = \exp(at). \quad (15)$$

The nonideality of radio-frequency pulses, the spread of fields, and the addition of other perturbing Hamiltonians to the main Hamiltonian [10, 11, 27, 29] lead to an incomplete time reversal and cause cluster degradation due to the loss of coherence (relaxation). The above processes inhibit the growth of \bar{K} . On this basis, in [11] it was proposed to control the growth of the number of correlated spins \bar{K} through a controlled small perturbation added to H_{DQ} at the preparation stage:

$$H_1 = (1-p)H_{DQ} + pH_{dd}. \quad (16)$$

Here, H_{dd} and H_{DQ} are the Hamiltonian specified by Eqs. (2) and (3), $|p| \ll 1$.

In [11] the number \bar{K} was extracted from the width of the experimental MQ spectrum by assuming that the relations derived in the ideal case could be used in the presence of a perturbation. However, the latter requires (as we noted in the Introduction) a justification, since the perturbation can change the shape of the MQ spectrum.

For example, in [24] it was experimentally established that the interaction H_{dd} causes a relaxation of the components of the MQ spectrum whose rate depends on both \bar{K} and M . In [49] we showed that this relaxation is due to local dipole fields and is representable by a product of two cofactors from two contributions to the local field:

$$\exp(-\bar{K}B^2t_d^2/2)\exp(-A^2M^2t_d^2). \quad (17)$$

Here, t_d is the duration of the evolution interval located between the preparation and mixing intervals. The parameter B^2 characterizes the uncorrelated contribution to the local field on each of the cluster spins that does not depend on the local field on other spins. In contrast, the parameter A^2 characterizes the cluster-averaged field acting in a correlated way on all cluster spins. Note that the constants A and B and their relationship can change in a wide range, since this depends on the form of the perturbation and the properties of the spin system. The first of the cofactors can indeed lead to a limitation of the growing-cluster sizes. Its manifestation was considered in [29, 31]. The influence of the second cofactor manifested itself, in particular, in the narrowing of the MQ spectrum observed in [26]. The result of the impact of the second component in Eq. (17) is realized in a more complex way. Below, we will consider its influence on the spectrum and the cluster size.

Since the perturbation in (16) is assumed to be small ($p \ll 1$), we will take into account its action phenomenologically by adding the relaxation factor to the distribution $P(K, T)$ in relation (9) and by supposing that the perturbation will not affect directly the TCFs $\{A_j(t)\}$ and the vectors $\{|j\rangle\}$. In accordance with the results of [33–35, 49]), we will this factor as a product of two cofactors:

$$\Gamma_{KM}(T) = \exp(-Kp^2B^2t_T^2/2)\exp(-p^2A^2M^2t_T^2) \quad (18)$$

$$= F_K(t)F_M(t),$$

$$t_T^2 = \langle (T-t)^2 \rangle = \int_0^T (T-t)^2 R(t) dt. \quad (19)$$

Here, the symbol $\langle \dots \rangle$ denotes an averaging over the coherence “emergence” time, t_T is the averaged coherence emergence time on the interval $[0, T]$, and $R(t)$ is some probability density characterizing the coherence emergence process:

$$R(t) = (dK(t)/dt)/K(T), \quad K(T) = K.$$

The relaxation factor of Eq. (18) differs from Eq. (17) due to the difference between the schemes of the corresponding experiments. In the situation described by Eq. (17), the growth of a cluster with an average size \bar{K} under the action of H_{DQ} and its decay under the action of H_{dd} occur sequentially, whereas in the case specified by Eq. (18), in the preparation period both processes occur in parallel. We take into account the fact that clusters of different sizes K grow and each such cluster has its own relaxation factor (18). For an exponential growth of the number of correlated spins in a cluster with $K(T) = K$, we will find for it:

$$K(t) = \exp(a_K t), \quad a_K = \frac{1}{T} \ln K, \quad (20)$$

$$\langle (T-t)^2 \rangle = \frac{2}{a_K^2} - \frac{2T}{a_K K(T)} - \frac{T^2}{K(T)}. \quad (21)$$

Relations (18)–(21) were derived by neglecting the contribution from the initial number of spins in the cluster. The decay, given the initial value of $K(0) = 1$, is considered in the Appendix.

Thus, given the cluster degradation processes, the shape of the MQ spectrum may be written as the following series [35]:

$$G_M(T) = \sum_{K=M}^{\infty} g_{KM} F_M(T) F_K(T) P(K, T) / N_1(T). \quad (22)$$

Here, $N_1(t)$ is the normalization factor,

$$N_1(T) = \sum_M \sum_{K=M}^{\infty} g_{KM} F_M(T) F_K(T) P(K, T). \quad (23)$$

For the average cluster size $\bar{K}(T)$, given the decay, instead of the series (11) we obtain the series

$$\bar{K}(T) = \sum_{K=1}^{\infty} K F_K(T) F_{\langle M \rangle}(K, T) P(K, T) / N_2(T), \quad (24)$$

where

$$N_2(T) = \sum_{K=1}^{\infty} F_K(T) F_{\langle M \rangle}(K, T) P(K, T) \quad (25)$$

is the normalization factor and

$$F_{\langle M \rangle}(K, T) = \sum_{M=K}^{M=K} g_{KM} F_M(T) \quad (26)$$

is the decay of a cluster of K spins averaged over M .

Choosing for large clusters g_{KM} in the form of a Gaussian function,

$$g_{KM} = \frac{1}{\sqrt{\pi K}} \exp\left(-\frac{M^2}{K}\right) \quad (27)$$

and replacing the summation in (26) by integration, we will find the M -averaged decay of a cluster of K spins (we neglect the boundary effects):

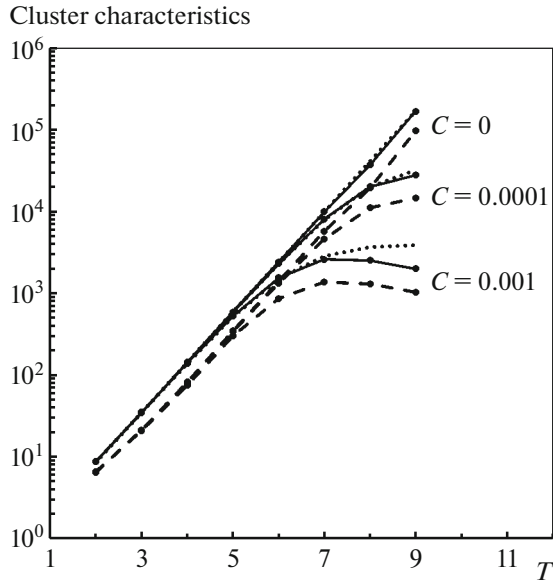


Fig. 1. Dependences of the characteristics of an average correlated spin cluster on preparation time T . The time is in units of $1/\sqrt{m_2}$. $\bar{K} = 2\langle M^2 \rangle$ (solid lines); M_e^2 (Eq. (34)) (dashed lines). The dotted lines indicate the dependences of \bar{K} calculated from Eq. (35). The figure presents the results of our calculations for $\alpha = 0$ and three values of the parameter C .

$$F_{\langle M \rangle}(K, T) = \int_{-\infty}^{\infty} g_{KM} F_M(T) dM \quad (28)$$

$$= [1 + KA^2 \langle (T-t)^2 \rangle]^{-1/2},$$

and the second moment of the MQ spectrum for the cluster of K spins:

$$\langle M^2 \rangle_K = \int_{-\infty}^{\infty} M^2 g_{KM} F_M(T) dM \quad (29)$$

$$= K[1 + KA^2 \langle (T-t)^2 \rangle]^{-3/2} / 2.$$

After the proper allowance for the decay of small clusters (see the Appendix) and relation (28) for the average cluster size $\bar{K}(T)$, we arrive at the expression

$$\bar{K}(T) = \exp(-A^2 T^2) \frac{P(1, T)}{N_3(T)} \quad (30)$$

$$+ \sum_{K=2}^{\infty} K F_K(T) [1 + KA^2 \langle (T-t)^2 \rangle]^{-1/2} \frac{P(K, T)}{N_3(T)},$$

$$N_3(T) = \exp(-A^2 T^2) P(1, T) \quad (31)$$

$$+ \sum_{K=2}^{\infty} F_K(T) [1 + KA^2 \langle (T-t)^2 \rangle]^{-1/2} P(K, T),$$

where $N_3(t)$ is the normalization.

At the same time, for the second moment of the MQ spectrum $G_M(T)$ (22) in the approximation

adopted above and given relation (29), the series turns out to be different:

$$\langle M^2 \rangle = \frac{1}{2} \exp(-A^2 T^2) \frac{P(1, T)}{N_3(T)} \quad (32)$$

$$+ \frac{1}{2} \sum_{K=2}^{\infty} K F_K(T) [1 + KA^2 \langle (T-t)^2 \rangle]^{-3/2} \frac{P(K, T)}{N_3(T)}.$$

Consequently, in the presence of M -dependent degradation processes, the series for the average number of spins $\bar{K}(T)$ (30) and the second moment $\langle M^2 \rangle$ (32) do not coincide. They differ by the exponents of the factor $[1 + KA^2 \langle (T-t)^2 \rangle]$ in the contribution to the sum from the cluster of K spins. This exponent is $-1/2$ (of the average cluster degradation) in the former case and $-3/2$ (of the second cluster moment) in the latter case.

4. RESULTS OF OUR NUMERICAL CALCULATIONS AND THEIR DISCUSSION

The relations derived in the previous section represent the solution of the formulated problem on the change in the shape of the MQ spectrum and the average correlated spin cluster size due an existing perturbation. Since we fail to sum the series in general form, we performed numerical calculations. We calculated the MQ spectra (22), their second moments $\langle M^2 \rangle$ (32), and the average cluster sizes $\bar{K}(T)$ (30) for various preparation times T and parameters characterizing the decay:

$$C = p^2 B^2 / m_2, \quad \alpha = A^2 / B^2. \quad (33)$$

The summation of the series over the number of involved spins K was replaced by integration over K from $K = 2$ to $K = 10^5 - 10^6$. From the calculated MQ spectra (22) we found the coherences M_e at which the MQ spectrum decreased by a factor of e . The point is that in experiments the MQ spectrum is commonly assumed to be Gaussian (1), for which the average cluster size is determined precisely by this quantity:

$$\bar{K}_e = M_e^2. \quad (34)$$

The results of our calculations are presented in Figs. 1–3.

Figure 1 presents the results of our calculations for the situation where there is no cluster degradation dependent on the coherence order M . The value of $\alpha = 0$ corresponds to this situation. In this case, the series (30) and (32) coincide and, hence, $\bar{K} = 2\langle M^2 \rangle$.

The dependences of M_e^2 on the preparation time T follow the dependences of \bar{K} on T , but with some shift (in logarithmic coordinates). The shift occurred, because the shape of the MQ spectrum (22), which is a sum of Gaussian functions, differs from a simple Gaussian function, as can be seen from Fig. 2a. Note that the

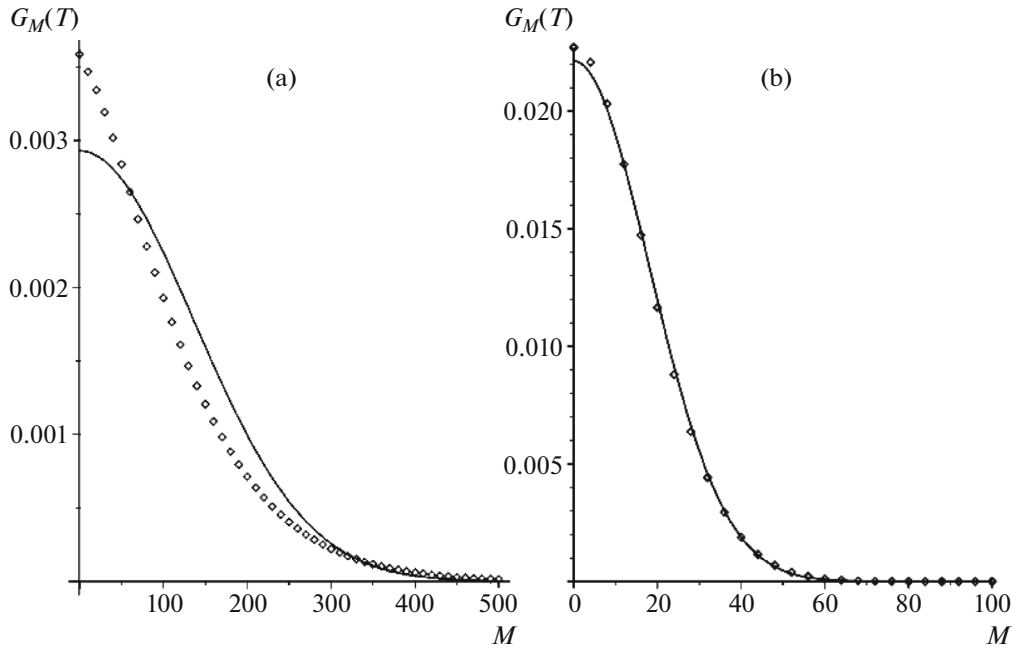


Fig. 2. (a) MQ NMR spectrum for the preparation time $T = 8/\sqrt{m_2}$ and $C = 0$. Only the right half is shown. The spectrum is symmetric relative to the vertical axis. The dots represent the results of our calculations using Eq. (22). The solid line indicates the Gaussian function $G_M(T) = (2\pi\langle M^2 \rangle)^{-1/2} \exp(-M^2/(2\langle M^2 \rangle))$ constructed for $2\langle M^2 \rangle = 37093.7m_2$ calculated from Eq. (32). (b) The same as Fig. 2a for $C = 0.0001$, $\alpha = 10$, and $2\langle M^2 \rangle = 650.16m_2$.

shape of the MQ spectrum in the complete absence of degradation processes (the ideal situation in which $C = 0$) was investigated in [37]. The spectrum was shown to be well described by a simple exponential observed previously in experiments [29].

It can be seen from Fig. 1 that at $C = 0$ there is an exponential growth of \bar{K} with T described by Eq. (14). Including extraneous perturbations causing cluster degradation dependent on the involved number of spins K slows down the growth of the number of spins \bar{K} at large T and entails the growth stopping. In [35], under the condition $\langle (T - t)^2 \rangle = 2/a^2$, we derived a formula for this case (rewritten here under the condition $a^2 = 2m_2$ and in the notation used now):

$$\bar{K}(T) = 1 + 2 \frac{\sinh^2(T/\sqrt{2}) \exp(-C/2)}{1 + \sinh^2(T/\sqrt{2})(1 - \exp(-C/2))}. \quad (35)$$

The corresponding dependences are indicated in Fig. 1 by the dotted lines for three values of the parameter C , and they describe the slowdown of the growth of \bar{K} at large T qualitatively correctly. Our calculations with a more complete (detailed) allowance for all the terms of relation (21) for $\langle (T - t)^2 \rangle$, including its dependence on K and T , lead to a greater limitation of \bar{K} at large T .

In the presence of degradation (decay) dependent on the coherence order M and changing the shape of

the MQ spectrum, the form of the cluster characteristics changes significantly with time T , as follows from Figs. 3a–3c. More specifically, the curves for the average cluster size determined by the following two methods diverge with increasing T :

- (1) from Eq. (30) as an average over the distribution of clusters in their \bar{K} changing with time $T(K)$;
- (2) from Eq. (34) through the total (average) MQ spectrum of clusters of different sizes $K(M_e^2)$.

In addition, twice the second moment of the MQ spectrum at small T is equal to \bar{K} , whereas at large T its value approaches M_e^2 . Such a behavior of the second moment is related to the change in the shape of the MQ spectrum. As follows from Fig. 2b, at $\alpha = 10$ and $c = 10^{-4}$ the shape of the MQ spectrum approaches the Gaussian one, whose width differs from \bar{K} and is close to M_e^2 . Finally, the dependences presented in Figs. 3a–3c demonstrate the existence of an interval of preparation times T in which the MQ spectrum is stabilized, while its characteristics M_e^2 and $\langle M^2 \rangle$ cease to grow, whereas the average cluster size \bar{K} continues to grow.

Thus, our calculations demonstrate the information about decoherence and scrambling obtained from the MQ NMR spectrum within the developed theory. For example, in the absence of decoherence, an

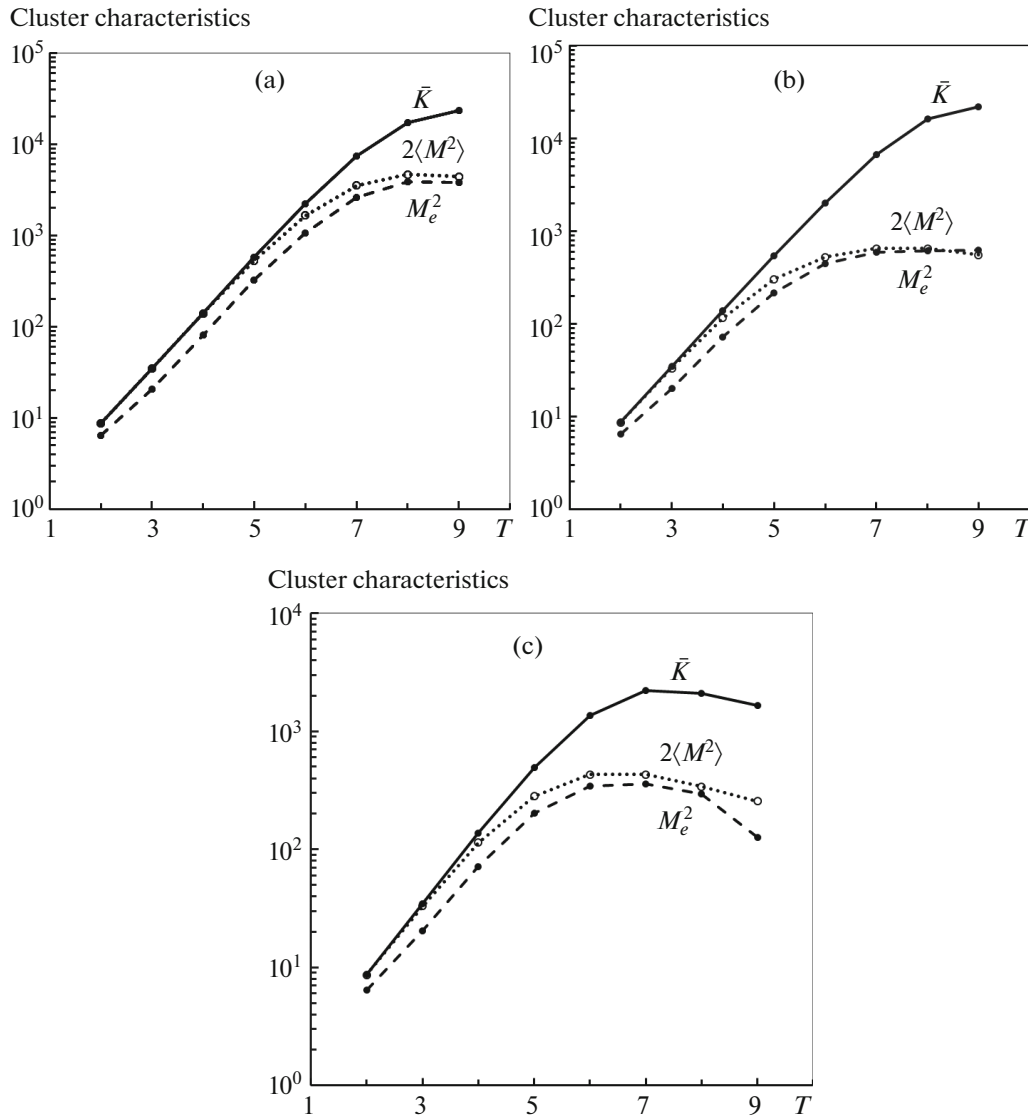


Fig. 3. The average number of spins in a cluster \bar{K} (Eq. (30), the solid line), the second moment of the MQ spectrum $2\langle M^2 \rangle$ (Eq. (32), the dotted line), and the number of spins in a cluster determined through the drop in the amplitude of the spectrum by a factor of $e M_e^2$ (Eq. (34), the dashed line) versus preparation time T . The time is in units of $1/\sqrt{m_2}$. The values of the parameters are: (a) $C = 0.0001, \alpha = 1$; (b) $C = 0.0001, \alpha = 10$; (c) $C = 0.001, \alpha = 1$.

unlimited exponential growth proportional to $\sinh^2(aT)$ of the width of the MQ spectrum with increasing preparation time T occurs as a result of the scrambling processes. The decoherence processes limit this growth as $T \rightarrow \infty$ by some limiting width of the MQ spectrum, whose qualitative dependence on the parameters can be represented by the following approximate formula [35]: $1/(p^2 B^2/2a^2 + 2p^2 A^2/a^2)$.

5. CONCLUSIONS

The model being developed allowed us to investigate the influence of the cluster degradation caused by

a controlled perturbation in the preparation period on the average size of a cluster of correlated spins, the shape of the MQ spectrum, and its second moment. Each of the quantities being calculated was represented as a sum of the weighted contributions from clusters of different sizes. The weights are the products of the occurrence probability of a cluster with coherence M and K spins by the function describing the degradation. We took into account both previously determined physical cluster degradation mechanisms: the rate of the first and the second ones is determined by the number of spins in the cluster and the coherence order, respectively. The first of these mechanisms

leads to a direct slowdown of the growth of the number \bar{K} with increasing time T and even to the stopping of the growth of the number of correlated spins \bar{K} (localization), as discussed in [11, 29–31] when justifying the method of controlling the spreading of quantum information through a controlled perturbation. The second mechanism changes the shape of the MQ spectrum and can lead to stabilization of the latter. The results of our calculations confirmed the following effect predicted by us previously [33–35]: when the MQ spectrum is stabilized, the growth of \bar{K} can continue. Thus, when applying MQ spectroscopy to study the spreading of quantum information, it is insufficient to measure the width of the MQ spectrum. It is necessary to elucidate the relationship between the rates of the two cluster degradation mechanisms caused by a perturbation in the object under study.

APPENDIX

In this Appendix we will consider in more detail the contribution from clusters of small sizes.

(1) The decay with an initial value of $K(0) = 1$.

$$F_K(T) = \exp \left\{ -\frac{B^2}{2} \left[K(0)T^2 + \int_0^T \frac{dK(t)}{dt} (T-t)^2 dt \right] \right\} \quad (\text{A.1})$$

$$= \exp(K(0)B^2T^2/2 - K(T)B^2t_T^2/2).$$

Since the initial contribution $\exp(K(0)B^2T^2/2)$ appears as a common factor for each term from the series (22) and (24) (and the corresponding series for the normalization factors (23) and (25), it cancels out after the normalization. For the first terms of the series (22) and (24) with $K = 1 = K(0)$ the cluster does not grow in the course of evolution. For them $dK(t)/dt = 0$ and there is no degradation (decay), i.e., $F_{K=1}(T) = 1$.

(2) The following simple formula was derived in the statistical model of the MQ spectrum for g_{KM} [6]:

$$g_{KM} = \begin{cases} \frac{1}{N_g} \binom{2K}{K-M}, & M \neq 0, \\ \frac{1}{2N_g} \left[\binom{2K}{K} - 2^K \right], & M = 0, \end{cases} \quad (\text{A.2})$$

where

$$N_g = 4^K - \frac{1}{2} \left[\binom{2K}{K} + 2^K \right]$$

is the normalization factor. Here, $\binom{n}{k}$ denotes a combinatorial factor: the number of combinations C_n^k . At $K = 1$ relation (A.2) leads to a doublet. At $K = 2$ g_{KM} consists of five lines. For large clusters the binomial shape of the MQ spectrum specified by relation (A.2) is replaced by a Gaussian function:

$$g_{KM} = \frac{1}{\sqrt{\pi K}} \exp \left(-\frac{M^2}{K} \right). \quad (\text{A.3})$$

(3) Consider the series (22) for the shape of the MQ spectrum at various values of M . At $M = 0$, according to (A.2), $g_{10} = 0$ and the series begins with the term for which $K = 2$:

$$G_{M=0}(T) = \sum_{K=2}^{\infty} g_{K0} F_K(T) P(K, T) / N_1(T).$$

Here, we took into account the fact that $F_{M=0}(T) = 1$.

At $M = \pm 1$ the series begins with $K = 1$:

$$G_{M=1}(T) = \frac{1}{2} F_{M=1}(T) F_{K=1}(T) P(1, T) / N_1(T) + \sum_{K=2}^{\infty} g_{K1} F_{M=1}(T) F_K(T) P(K, T) / N_1(T).$$

Here, $F_{K=1}(T) = \exp(-B^2T^2/2)$ is the initial contribution and $F_{M=1}(T) = \exp(-A^2T^2)$. In accordance with the assumption in our paper [49], these are the contributions from the nearest and far spins on only one cluster spin.

At $M \geq 2$ the series begins with $K = M \geq 2$.

Given what has been said above, in the series (22), (30), and (32) we single out the first term, while at $K \geq 2$ we choose g_{KM} in the form of a Gaussian function. In the function $F_K(T)$ from Eq. (A.1) the initial contribution is excluded, since it appears as a common factor for each term of the series and cancels out during the normalization.

FUNDING

This work was supported within the State assignment of the Ministry of Science and Higher Education of the Russian Federation (registration number 1021051201992-1).

CONFLICT OF INTEREST

The authors declare that they have no conflicts of interest.

REFERENCES

1. R. Ernst, G. Bodenhausen, and A. Wokaun, *Principles of NMR in One and Two Dimensions* (Clarendon, Oxford, 1987).
2. P.-K. Wang, J.-P. Ansermet, S. L. Rudaz, Z. Wang, S. Shore, Ch. P. Slichter, and J. M. Sinfelt, *Science* (Washington, DC, U. S.) **234**, 35 (1986).
3. J. Baum and A. Pines, *J. A. Chem. Soc.* **108**, 7447 (1986).
4. S. I. Doronin, A. V. Fedorova, E. B. Fel'dman, and A. I. Zenchuk, *J. Chem. Phys.* **131**, 104109 (2009).
5. J. Baum, M. Munovitz, A. N. Garroway, and A. Pines, *J. Chem. Phys.* **83**, 2015 (1985).
6. M. Munovitz and A. Pines, *Adv. Chem. Phys.* **6**, 1 (1987).

7. R. Balesku, *Equilibrium and Nonequilibrium Statistical Mechanics* (Wiley, New York, 1978), Vol. 2.
8. J. Preskill, *Lecture Notes for Physics*, Vol. 229: *Quantum Information and Computation* (California Inst. Technol., 1998).
9. V. E. Zobov and A. A. Lundin, *J. Exp. Theor. Phys.* **131**, 273 (2020).
10. C. M. Sanchez, A. K. Chattah, and H. M. Pastawski, *Phys. Rev. A* **105**, 052232 (2022).
11. F. D. Domínguez, M. C. Rodríguez, R. Kaiser, D. Suter, and G. A. Álvarez, *Phys. Rev. A* **104**, 012402 (2021).
12. S. H. Shenker and D. Stanford, *J. High Energy Phys.*, No. 3, 067 (2014).
13. D. E. Parker, X. Cao, A. Avdoshkin, T. Scaffidi, and E. Altman, *Phys. Rev. X* **9**, 041017 (2019).
14. Q. Wang and F. Perez-Bernal, *Phys. Rev. A* **100**, 062113 (2019).
15. Y. Gu, A. Kitaev, and P. Zhang, *J. High Energy* **2022**, 133 (2022).
16. C. Gross and I. Bloch, *Science* (Washington, DC, U. S.) **357**, 995 (2017).
17. R. Blatt and C. F. Roos, *Nat. Phys.* **8**, 277 (2012).
18. A. K. Khitrin, *Chem. Phys. Lett.* **274**, 217 (1997).
19. V. E. Zobov and A. A. Lundin, *J. Exp. Theor. Phys.* **103**, 904 (2006).
20. M. Gärttner, Ph. Hauke, and A. M. Rey, *Phys. Rev. Lett.* **120**, 040402 (2018).
21. S. I. Doronin, E. B. Fel'dman, and I. D. Lazarev, *Phys. Rev. A* **100**, 022330 (2019).
22. S. I. Doronin, E. B. Fel'dman, and I. D. Lazarev, *Phys. Lett. A* **406**, 127458 (2021).
23. K. X. Wei, P. Peng, O. Shtanko, I. Marvian, S. Lloyd, C. Ramanathan, and P. Cappellaro, *Phys. Rev. Lett.* **123**, 090605 (2019).
24. H. G. Krojanski and D. Suter, *Phys. Rev. Lett.* **93**, 090501 (2004).
25. H. G. Krojanski and D. Suter, *Phys. Rev. Lett.* **97**, 150503 (2006).
26. H. G. Krojanski and D. Suter, *Phys. Rev. A* **74**, 062319 (2006).
27. G. A. Álvarez and D. Suter, *Phys. Rev. Lett.* **104**, 230403 (2010).
28. G. Cho, P. Cappellaro, D. G. Cory, and C. Ramanathan, *Phys. Rev. B* **74**, 224434 (2006).
29. G. A. Álvarez and D. Suter, *Phys. Rev. A* **84**, 012320 (2011).
30. G. A. Álvarez, D. Suter, and R. Kaiser, *Science* (Washington, DC, U. S.) **349**, 846 (2015).
31. F. D. Domínguez and G. A. Álvarez, *Phys. Rev. A* **104**, 062406 (2021).
32. D. Levy and K. Gleason, *J. Phys. Chem.* **96**, 8125 (1992).
33. V. E. Zobov and A. A. Lundin, *J. Exp. Theor. Phys.* **113**, 1006 (2011).
34. A. A. Lundin and V. E. Zobov, *Appl. Magn. Res.* **47**, 701 (2016).
35. V. E. Zobov and A. A. Lundin, *Appl. Magn. Res.* **52**, 879 (2021).
36. M. H. Lee, I. M. Kim, W. P. Cummings, and R. Dekeyser, *J. Phys.: Condens. Matter* **7**, 3187 (1995).
37. A. A. Lundin and V. E. Zobov, *J. Exp. Theor. Phys.* **120**, 762 (2015).
38. A. Abragam, *The Principles of Nuclear Magnetism* (Clarendon, Oxford, 1961), Chap. 4, 10.
39. R. H. Schneder and H. Schmiedel, *Phys. Lett. A* **30**, 298 (1969).
40. W. K. Rhim, A. Pines, and J. S. Waugh, *Phys. Rev. B* **3**, 684 (1971).
41. F. Lado, J. D. Memory, and G. W. Parker, *Phys. Rev. B* **4**, 1406 (1971).
42. M. H. Lee, *Phys. Rev. Lett.* **52**, 1579 (1984).
43. M. H. Lee and J. Hong, *Phys. Rev. B* **32**, 7734 (1985).
44. J. M. Liu and G. Müller, *Phys. Rev. A* **42**, 5854 (1990).
45. V. L. Bodneva, A. A. Lundin, and A. A. Milyutin, *Theor. Math. Phys.* **106**, 370 (1996).
46. M. Böhm, H. Leschke, M. Henneke, et al., *Phys. Rev. B* **49**, 5854 (1994).
47. V. A. Il'in and G. D. Kim, *Linear Algebra and Analytic Geometry* (Mosk. Gos. Univ., Moscow, 2008), Chap. 13 [in Russian].
48. A. A. Lundin and V. E. Zobov, *Russ. J. Phys. Chem. B* **40**, 839 (2021).
49. V. E. Zobov and A. A. Lundin, *J. Exp. Theor. Phys.* **112**, 451 (2011).

Translated by V. Astakhov